Analysis of Air-recirculation of Air-source heat pump evaporators using CFD simulations

1. Introduction

The present study investigates the effect of air recirculation on the average inlet air temperatures of an air-source heat pump. The evaporator is generally composed of air intakes (the air is entrained into the evaporator, by a fan), a heat exchanger (fin & tubes) and an exhaust where the air leaves the evaporator. In the case of an air-source heat pump for district heating, heat from the ambient air is absorbed by the refrigerant in the heat exchanger, leading to a colder exhaust stream compared to the ambient air temperature. A simple 3D model of an evaporator is shown in Figure 1.

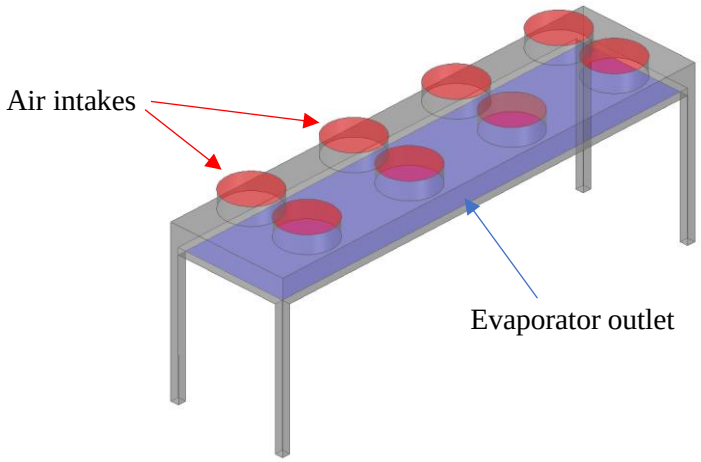

Figure 1. Simplified 3D model of an horizontal evaporator, with 8 intakes and 1 exhaust

For evaporators subject to outdoor conditions, the influence of the wind speed and wind direction has to be investigated, since it might affect the average inlet air temperature, which affects the performance of the evaporator, and therefore the performances of the heat pump (in terms of COP). Figure 2 represents the flow behaviour around an evaporator for a wind blowing in the z direction.

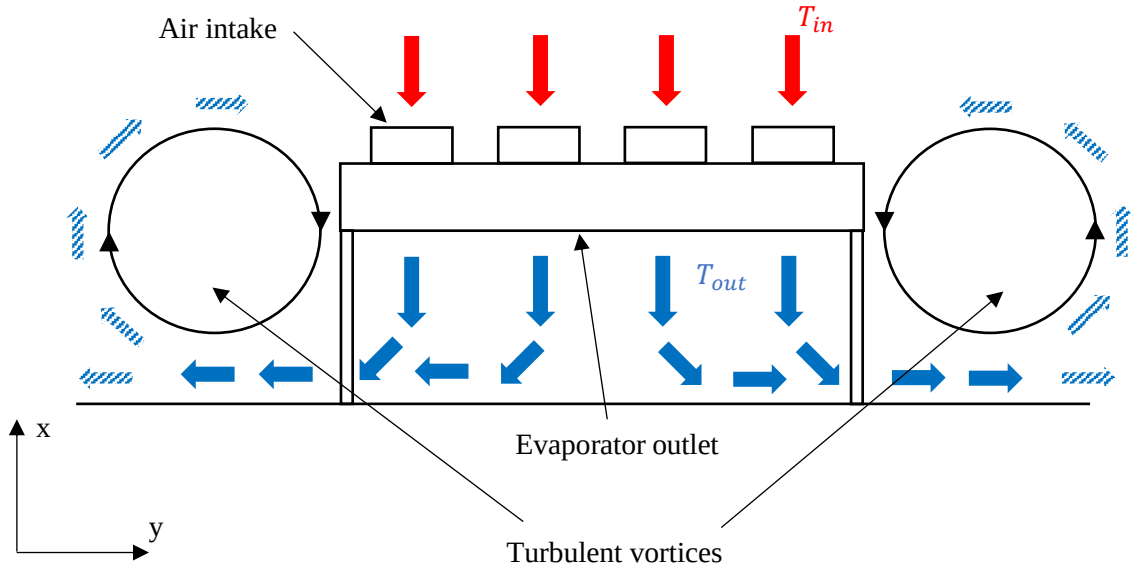

Figure 2. 2D sketch of flow recirculation around evaporator

The flow around the evaporator can be laminar or turbulent, depending on the ambient wind velocity, wind direction, fan speed of the evaporator, the presence of obstacle (e.g. evaporators legs), leading to the formation of turbulent vortices around the evaporator, as shown in Figure 2. These vortices will form secondary flow patterns and create recirculation. The recirculation is defined by the amount of cold air, entrained by the vortices, circulating back to the intakes of the evaporator. The recirculation ratio can be defined by the following equation:

$$\varphi = 1 - \frac{T_{in} - T_{out}}{T_{\infty} - T_{out}} \quad (1)$$

A ratio $\varphi = 0$ ($T_{in} = T_{\infty}$) corresponds to no recirculation, when $\varphi = 1$ ($T_{in} = T_{out}$) corresponds to a full recirculation.
Additionally to the flow speed velocity and direction, the vortices' sizes, intensity and locations vary with respect to the size and the number of evaporators. The vortices may appear small at the start of the evaporator and increase in size along the main flow direction.
Given the complexity of the flow structure, and the number of parameters involved, a CFD approach seems to be a suitable tool to give a good understanding of the recirculation effect. However, several assumptions have to be made in order to keep the CFD simulation feasible and not too time consuming.

2. CFD modelling of the evaporator

First, a CFD model of a single evaporator is carried out as a proof-of-concept (PoC). In a second hand, the CFD model is extended to model the test case of the air-source heat pump located in the Danish city of Brædstrup. The Brædstrup heat pump is composed of 20 horizontal evaporators placed on a single line. Each evaporator is composed of eight air intakes and a single one outlet. The dimensions are based on the AlphaLaval Lu-Ve BD-1000 evaporator used for the Brædstrup heat pump, and are summarized in the Table 1.

Table 1. Dimensions of the AlphaLaval Lu-Ve BD-1000 evaporator

Length (mm)	Width (mm)	Height (mm)	Heat-exchanger height (mm)	Intake height (mm)	Intake diameter (mm)
8450	2250	4120	490	330	1080

The initial CFD model of a single evaporator is based on the AlphaLaval Lu-Ve BD-1000.

2.1. Modelling assumptions

Several modelling assumption have been chosen to model the flow around the evaporator. First, inner geometries of the evaporator, such as the fins and tubes of the heat exchanger and the fans, are disregarded. Modelling the whole geometry would require an extensive amount of mesh nodes to cover the broad range of scale, from the order of millimetres (fins) to decametres (buildings).
The evaporator is therefore modelled as a "black-box" with inlets, corresponding to the intake of the air entrained by the fans, and an outlet, corresponding to the exhaust of the heat exchanger. The assumptions used in the CFD model are:

- The swirl generated by the fans is not accounted. However, it is assumed that the flow entering the heat exchanger will become mostly uni-directional due to the restriction of the free flow area in the fins and tubes region.
- No pressure drop is modelled along the fans and the heat exchanger. Whereas this assumption will lead to large uncertainties in the prediction of the performances of the heat exchanger itself, it is believed that the recirculation ratio will not be affected by it. Pressure variation will be only a result of the flow motion around the evaporator.
- The heat exchanger is modelled by a temperature drop of 4 K between the ambient air temperature and the evaporator's outlet temperature. The performances of the heat exchanger are not of interest in this study, only the recirculation ratio.

The results of this study will help heat pump designers to optimize the placement of the evaporators to reduce the recirculation as much as possible. The recirculation ratio calculated by the CFD model can be used to account for the loss in the evaporator performances in another 0D or 1D system model of the whole heat pump.

2.2. 3D model and calculation domain

The 3D model of the evaporator is placed in a larger domain to model the flow around the evaporator. Considering the large size of the evaporator, especially in the case of multiple devices placed side by side such as in the Brædstrup case, the general guidelines for CFD simulation of flows in the urban environment have been applied. These guidelines are found in the work of Franke et al. [1] who defined "rules" on how to model flows around large obstacles (e.g. buildings) considering domain size, mesh strategies, appropriate boundary conditions, turbulence models, etc.

- Domain size

The domain around the evaporator has to be expended in all direction to properly model the flow around the obstacle. Considering a building height H, the blockage ratio in the flow direction should be inferior to 3%, based on experience of wind tunnel experiments and CFD simulations. The blockage ratio corresponds to the ratio of the projected area of the obstacle in the flow direction to the cross-section area of the domain in the flow direction.

$$B = \frac{A_{obstacle}}{A_{domain}} \tag{2}$$

The vertical extension should be at least $5H$ to avoid any artificial acceleration of the flow since upper boundary conditions generally do not allow the flow to leave the domain (similar to wind tunnel experiments). On lateral directions, the factor n for the extended length nH is chosen to respect the minimum blockage ratio of 3%. In the flow direction, upstream, the distance can be reduced to $2H$ if the ground topology is flat. The inlet boundary conditions will be modified to include the effect of the wind boundary layer. Finally the extension in the flow direction, downstream, is the largest with $15H$ to allow re-development of the flow in the wake region. The boundary condition at the outlet is chosen to allow flow entering back to the domain so to ensure no influence on the boundary type.

- Boundary conditions

The **inlet boundary conditions** is a velocity inlet type, with a specified velocity profile to account for the effect of the boundary layer. Thus allows to considerably reduce the domain size upstream of the evaporator and assuring a physical representation of the wind profile. The profile is determined by a preliminary 2D CFD simulation, where the inlet and outlet are presumed periodic. The mass flow rate between the inlet and the outlet is calculated to give a desired average velocity. The inlet wind is therefore assumed 2D (no variation in lateral direction) which is a valid assumption if the ground is free of obstacles upstream of the evaporator. The velocity profile is show in Figure 3, for an average velocity of 3.7 m/s.

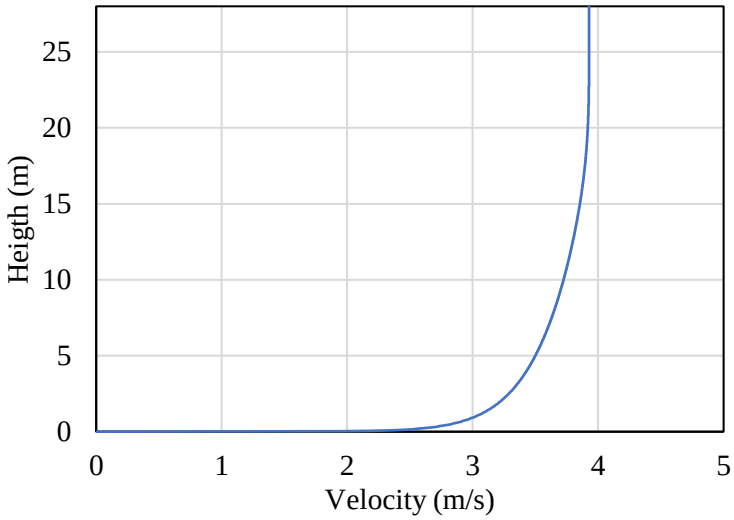

Figure 3. Inlet velocity profile in function of the height of the domain

The **outlet boundary condition** is a constant static pressure boundary conditions where recirculation of the flow back to the domain is allowed, to account for the formation of vortices far away from the obstacle. **Lateral and upper boundary conditions** are symmetry. This forces the flow to be strictly parallel to the main flow direction at the boundaries. This is true only at a location far away from the obstacles, if the main flow direction is aligned with the geometrical axis of the domain. The ground and the evaporator's walls are considered as **no-slip adiabatic walls**.
Finally the air intake is modelled as a mass flow outlet (the flow **leaves** the domain, at 4 kg/s) and the outlet of the evaporator as a mass flow inlet (the flow **enters** the domain, at 4 kg/s) at a constant temperature T_{out}. The difference in the mass flow rates is assured to be zero to ensure mass balance.
The fluid is assumed incompressible since the diffusive heat transfer is much more important than the natural convection due to the change of fluid's density.

- Meshing

The mesh is built to capture the complexity of vortex formation in the domain. An inflation layer is applied on the ground level with a $y^+ > 30$, corresponding to the use of realizable k-ε turbulence model. The mesh is locally refined close the evaporator, and slowly increase in size along all directions. The mesh is also fully structured to avoid numerical diffusion.

2.3. Results

The inputs of the CFD simulation are summarized in the Table 2. The wind is blowing towards the front of the evaporator.

Table 2. Boundary conditions of the CFD model

Velocity inlet (m/s)	Temperature inlet (°C)	Pressure outlet (Pa)	Intake mass flow rate (kg/s)	Intake temperature (°C)	Exhaust mass flow rate (kg/s)
3.7	8.9	0	-32	4.9	32

The inlet average velocity and temperature correspond to the average velocity and temperature for the last 10 years at the city of Horsens, the closest city with available data from DMI (Danmarks Meteorologiske Institut). These average values also correspond to the most prevalent wind and temperature conditions at any given day (expect during the peak of winter and summer),
The Figure 4 and Figure 5 represent the velocity streamlines and temperature contour at different cross-sections of the evaporator. The wind direction is represented by a blue large arrow.

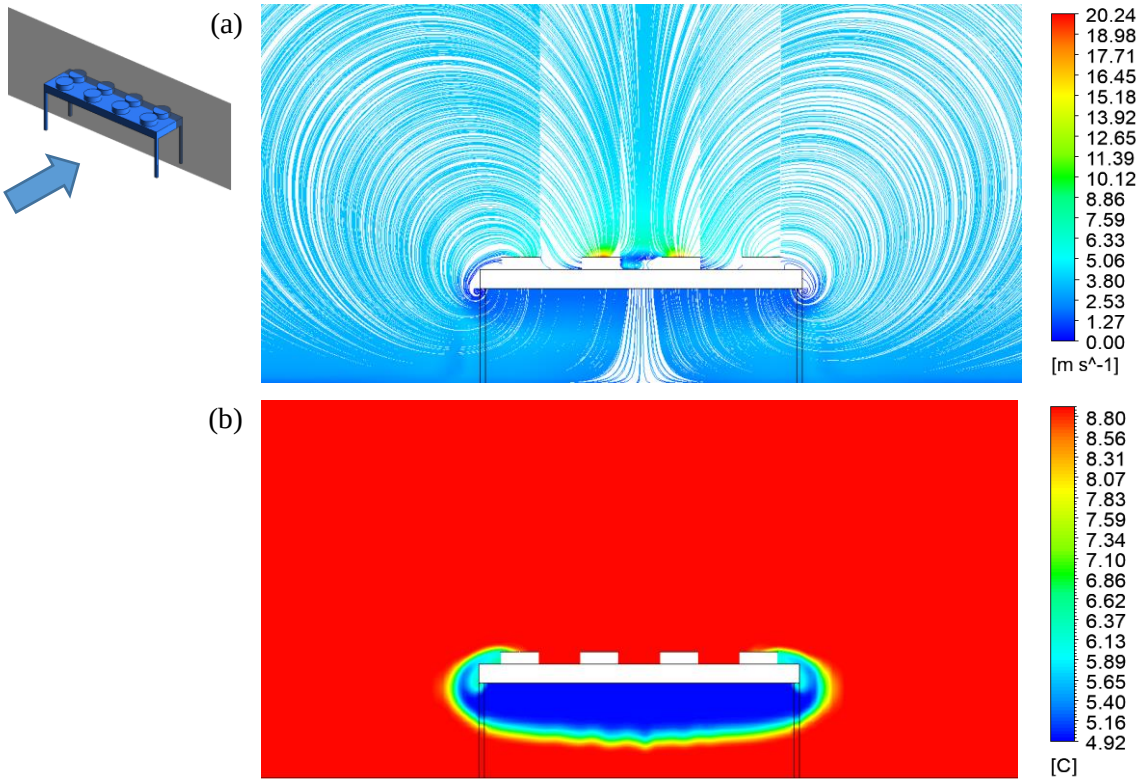

Figure 4. In-plane velocity streamlines (a) and temperature contour (b) at frontal cross-section of the evaporator, for one evaporator

The recirculation is characterized by the two vortices at both sides of the evaporator. The cold air, flowing toward the ground from the evaporator's exhaust, is entrained by the vortices and directed back to the evaporator's intakes. The temperature plot (b) shows that only the lateral fans are impacted by the recirculation. The suction of the air by the lateral evaporator's intakes prevent the cold air to reach the inner intakes.

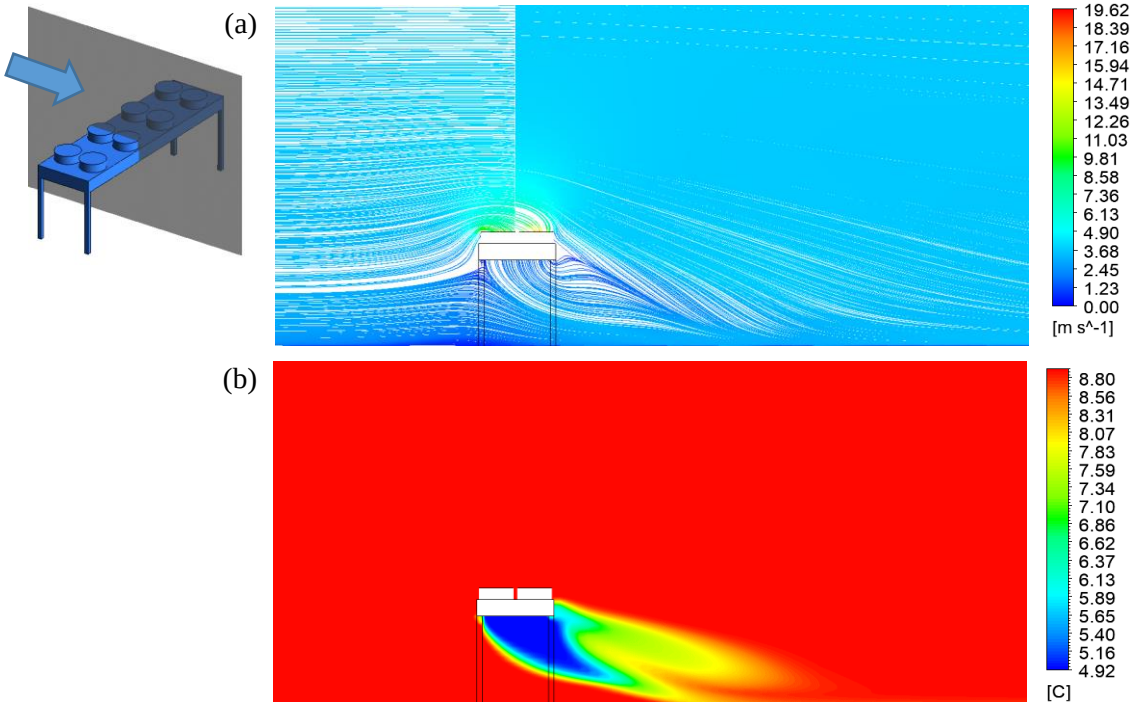

Figure 5. In-plane velocity streamlines (a) and temperature contour (b) at lateral cross-section of the evaporator, for one evaporator

The streamlines show that the cold air is pushed towards the ground along the flow direction. However, due to the mixing, the exhaust air temperature rapidly increases back to the ambient air temperature. The temperature profile of the evaporator walls is shown in Figure 6.

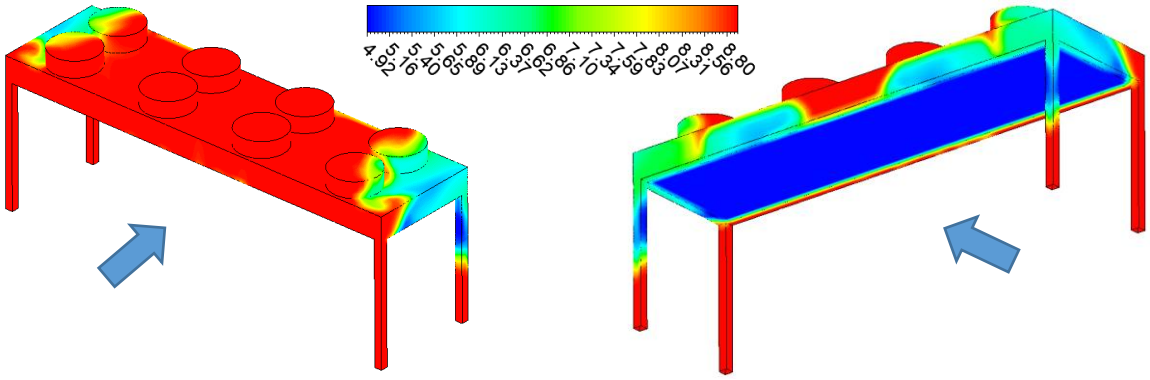

Figure 6. Temperature contour of the outer evaporator wall, for one evaporator

The recirculation increases along the flow direction, due to an increase in vortices' size and strength. However, for a single evaporator, the recirculation ratio remain small with φ = 7.8%.
The next section focuses on the Brædstrup case with a higher number of evaporators.

3. Brædstrup test case with "perfect" field

The air-source heat pump of Brædstrup is composed of 20 evaporators placed in-line. The evaporators are joined by group of 2, with a short distance of 0.6 m between two consecutive groups, to allow human maintenance. A 3D model of the 20 evaporators is shown in Figure 7.

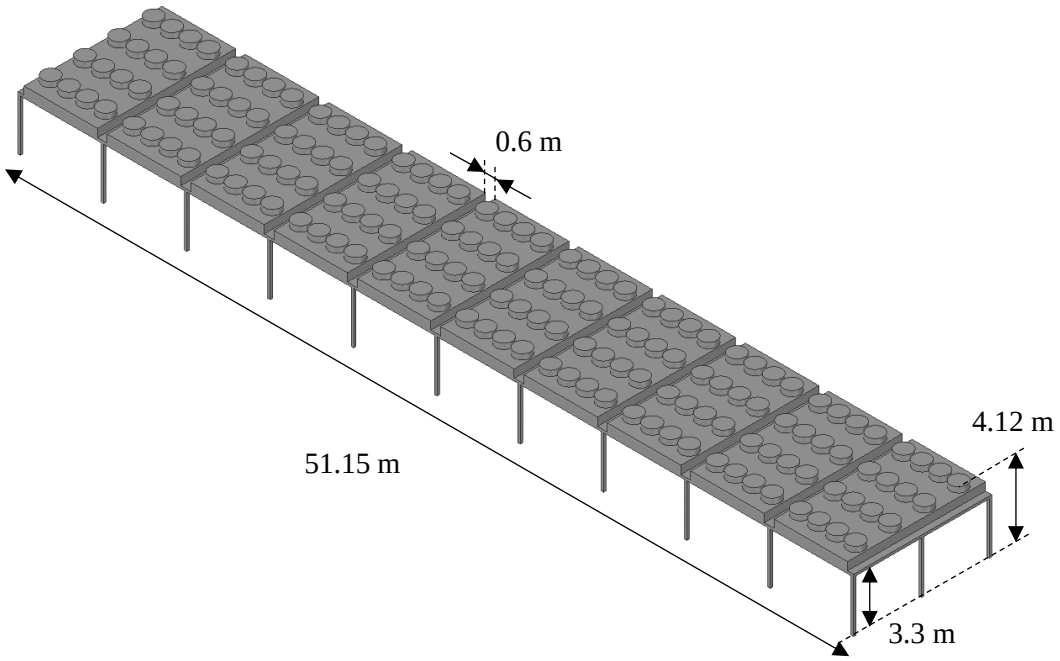

Figure 7. 3D model of the Brædstrup 20 evaporators

The boundary conditions of the CFD simulation for a single evaporator have been used for the 20 evaporators' case. The mass flow rates have been increased to 32x20 = 640 kg/s for both intakes and exhausts.
The evaporator's have two symmetry planes. Thus meaning that it is possible to determine the influence of the wind direction on the recirculation ratio, by limiting the wind angle change by 90° in the

simulations instead of 360°. Therefore, 5 simulations have been carried out for 5 wind directions within the 90° angle range: south (S) to east (E) with three intermediate angles separated by 22.5 degrees, as shown in Figure 8. The wind speed and ambient temperature are not changed.

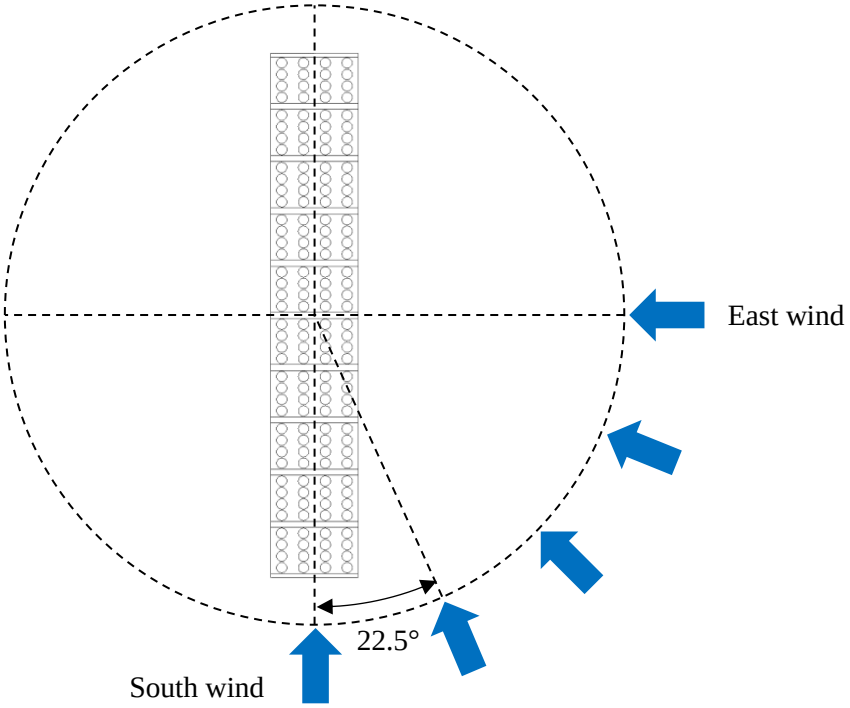

Figure 8. Sketch of the 20 evaporators under different wind conditions in the CFD simulations

The size of domain is updated in function of the wind direction, to account for the change of the flow frontal area of the evaporators. The mesh size of all configurations ranges from 24 to 26 M nodes. The simulations are carried out using 32 cores of an Intel Xeon CPU E5-2670 @ 2.6 GHz and 64 GB of RAM. The simulation time is approximately 2 days for 20000 iterations.

3.1. South wind

First, the simulation for a south wind direction has been carried out. In the same way than for the single evaporator case, the streamlines at different cross-sections have been plotted in Figure 9.

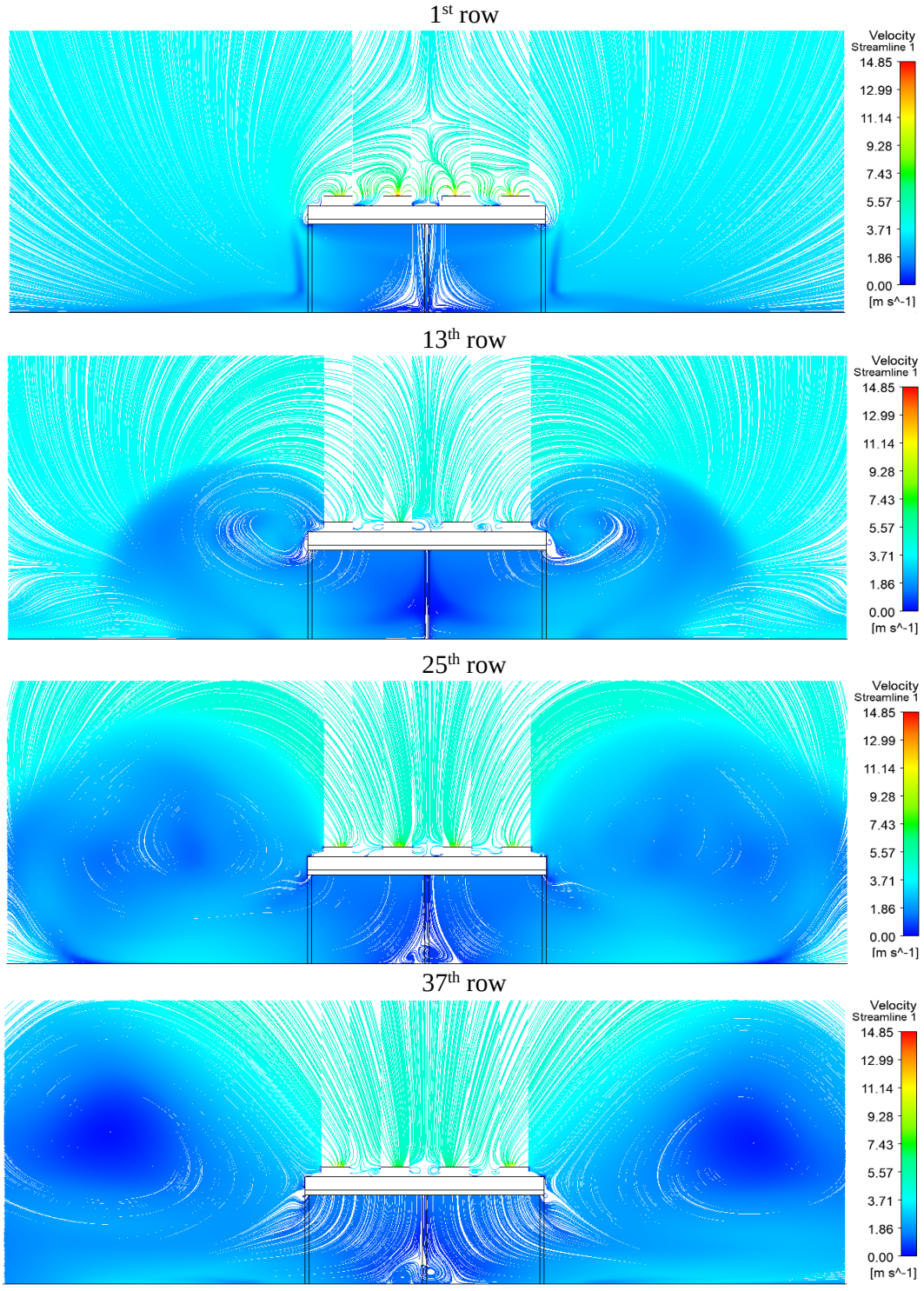

Figure 9. In-place velocity streamlines at different locations (rows) of the evaporators, for 20 evaporators and south wind condition

The vortices grow in size as the air flows downstream, and move away from the evaporators' lateral sides. The associated temperature contour at the same locations is shown in Figure 10.

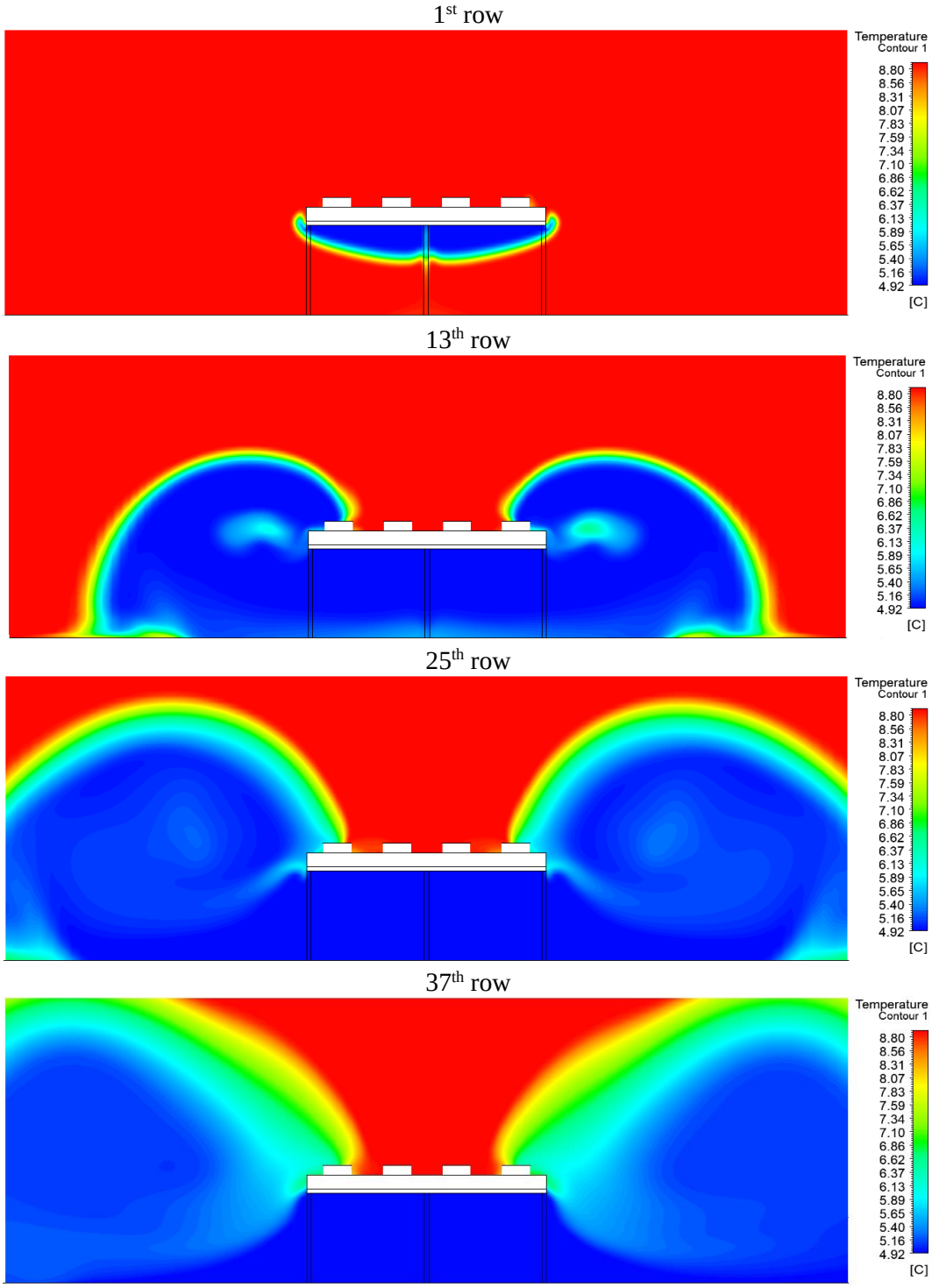

Figure 10. Temperature contour at different locations (rows) of the evaporators, for 20 evaporators and south wind condition

The recirculation affects only the lateral intakes, in the same manner as for the single evaporator case. The displacement of the vortices centres away from the evaporators' side can be seen in Figure 11 and Figure 12. The Figure 11 represents the vortices region of the domain, using the λ_2 method, whereas Figure 12 shows the location of the vortices centre along the flow direction. The λ_2 method was defined by Jeong and Hussain [2], and to sum up, represents the excess of rotation rate over the strain rate magnitude, on a specific plane. Therefore, the values of λ_2 can be shown by iso-surfaces for negative values of λ_2, which indicates the presence of vortices.

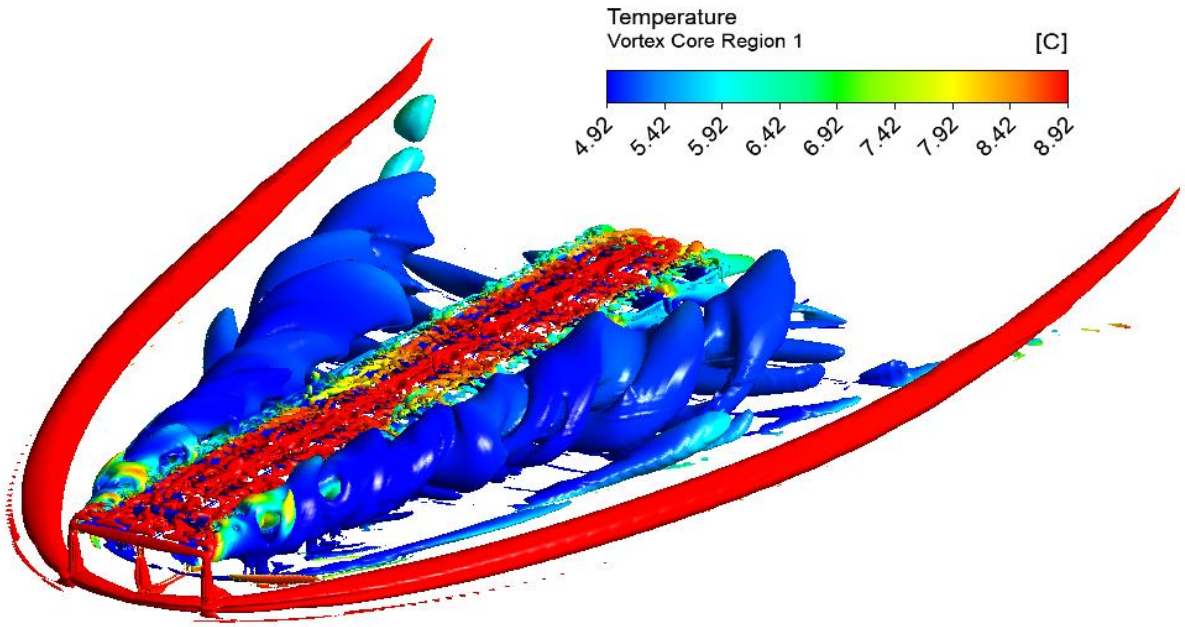

Figure 11. Vortices region of the flow around the evaporators with associated temperature field, for 20 evaporators and south wind condition

The horseshoe vortex (in red) is a typical vortex type encountered for flow around an obstacle. It represents the boundary region where the main flow is impacted by the presence of the obstacle. The vortex is red (ambient temperature), which indicates that there is no mixing of the ambient air and the colder flow leaving the exhaust of the evaporators in this region. On the other hand, the main vortices responsible for recirculation are shown in blue alongside the evaporators. It clearly shows that the cold air is entrained by the lateral vortices and recirculates back to the evaporators' intakes. The smaller red vortices on top of the evaporators are due to the presence of the rounded fan intakes, which disturb the flow in a lower magnitude.

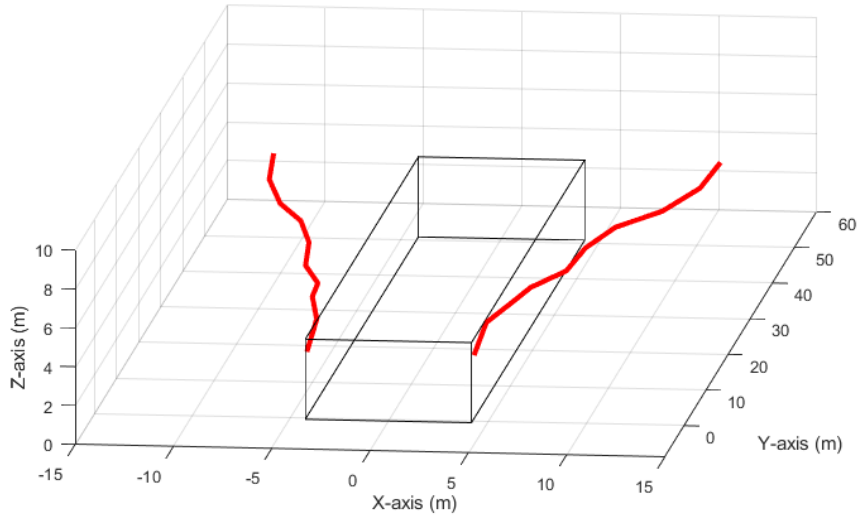

Figure 12. Location of the centres of lateral vortices along the flow direction (in red), for 20 evaporators and south wind condition

Figure 12 shows that the vortices moves apart of the evaporators in a linear way. The centres of the lateral vortices have the same height as the height of the evaporators. The resulting temperature contour of the evaporators is shown in Figure 12Figure 13.

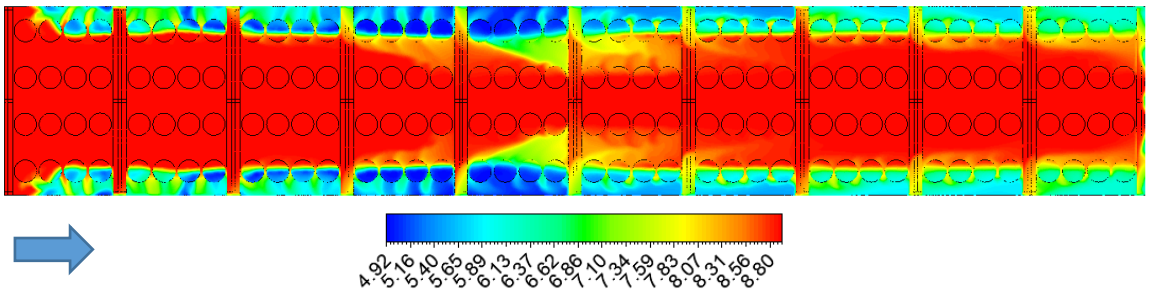

Figure 13. Temperature contour of the evaporators (top side), for 20 evaporators and south wind condition

The corresponding local recirculation ratio at the intakes of the evaporators is shown in Figure 14.

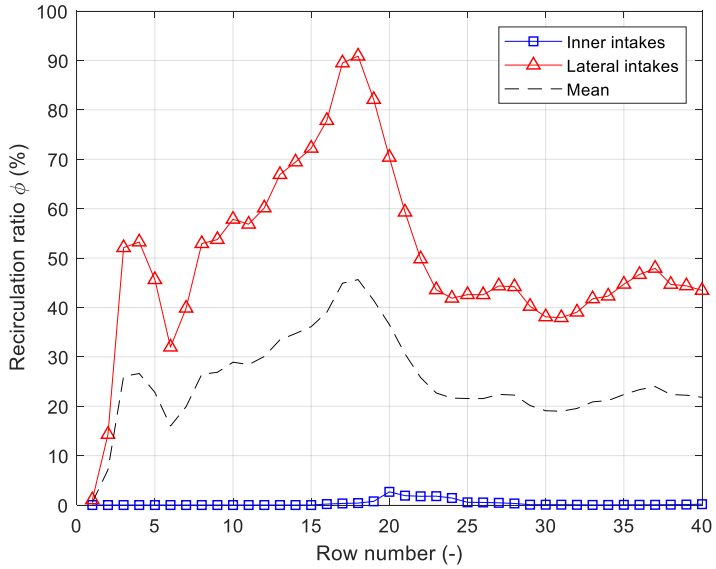

Figure 14. Local and mean recirculation at the intakes of the evaporators, for 20 evaporators and south wind condition

The recirculation appears at the second row of the fan inlets. The intensity increases along the flow direction according to the development of the vortices. However, the recirculation starts to decrease at the 18th row (9th evaporator), with a rapid increase of the temperature at the inlets. The recirculation remain rather constant from the 24th row until the last row.

The sudden decrease in recirculation ratio is due to the displacement of the lateral vortices away from the evaporators. This phenomenon can be partially explained by the loss of kinetic energy of the main flow below the evaporator's exhausts. At a certain distance from the start of the evaporator, the main flow does not have sufficient kinetic energy to entrain the exhaust flow downstream. The exhaust air starts to flow in all direction, pushing the vortices away from the evaporators. Figure 15 shows that the change of direction of the exhaust air starts at the 9th evaporator, corresponding to the local change of recirculation ratio. Finally, the average recirculation ratio for south wind condition is φ = 26.4 %.

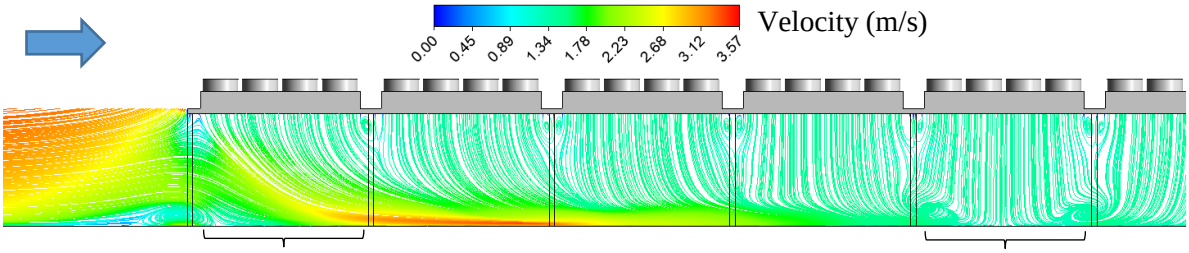

Figure 15. Velocity streamlines below the evaporators, for 20 evaporators and south wind condition

In this figure, we can clearly see that the main flow loses speed until the exhaust flow from the evaporators start to go in all direction. Having a different wind speed will certainly move the location where the exhaust air starts to flow in all direction.

3.2. East wind

The domain size has been updated and the same boundary conditions as the south wind case have been applied. The Figure 16 and Figure 17 show the velocity streamlines and temperature contour, at the same location as for the south wind case. The wind direction is from the right to the left.

The exhaust air is also entrained by the mean flow. However, the exhaust flow produces an adverse pressure gradient at the start of the evaporators (right side), which forces the main flow to recirculate above the evaporators. It is shown by the appearance of small vortices close to the ground (at 1st and 37th rows) at the start of the evaporators, or even a total blockage of the main flow if away from the evaporators' lateral edges (at 13th and 25th rows). As already explained in the previous section, the main flow does not have enough kinetic energy to entrain the mass of air leaving the evaporators at the exhaust.

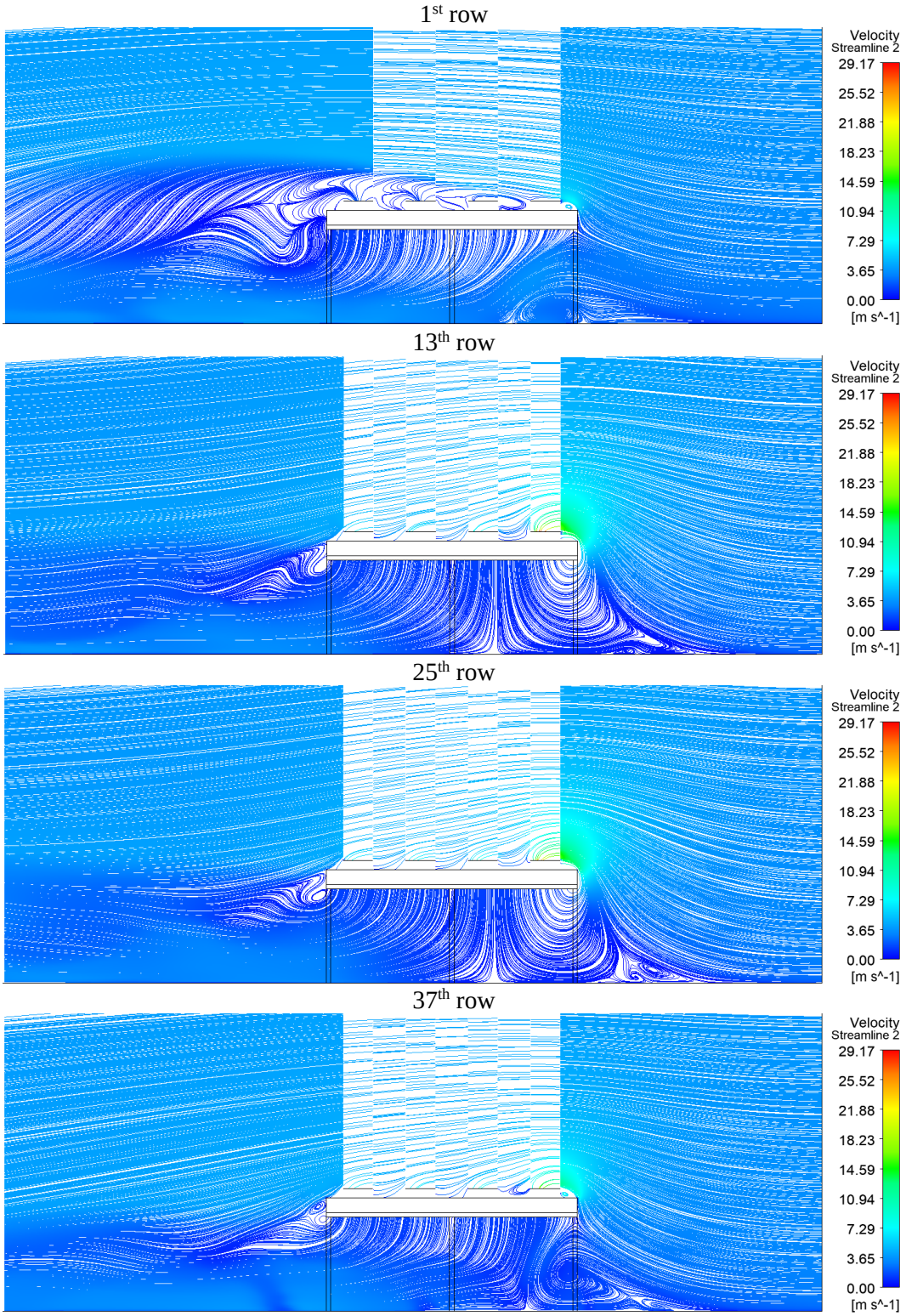

Figure 16. In-place velocity streamlines at different locations (rows) of the evaporators, for 20 evaporators and east wind condition

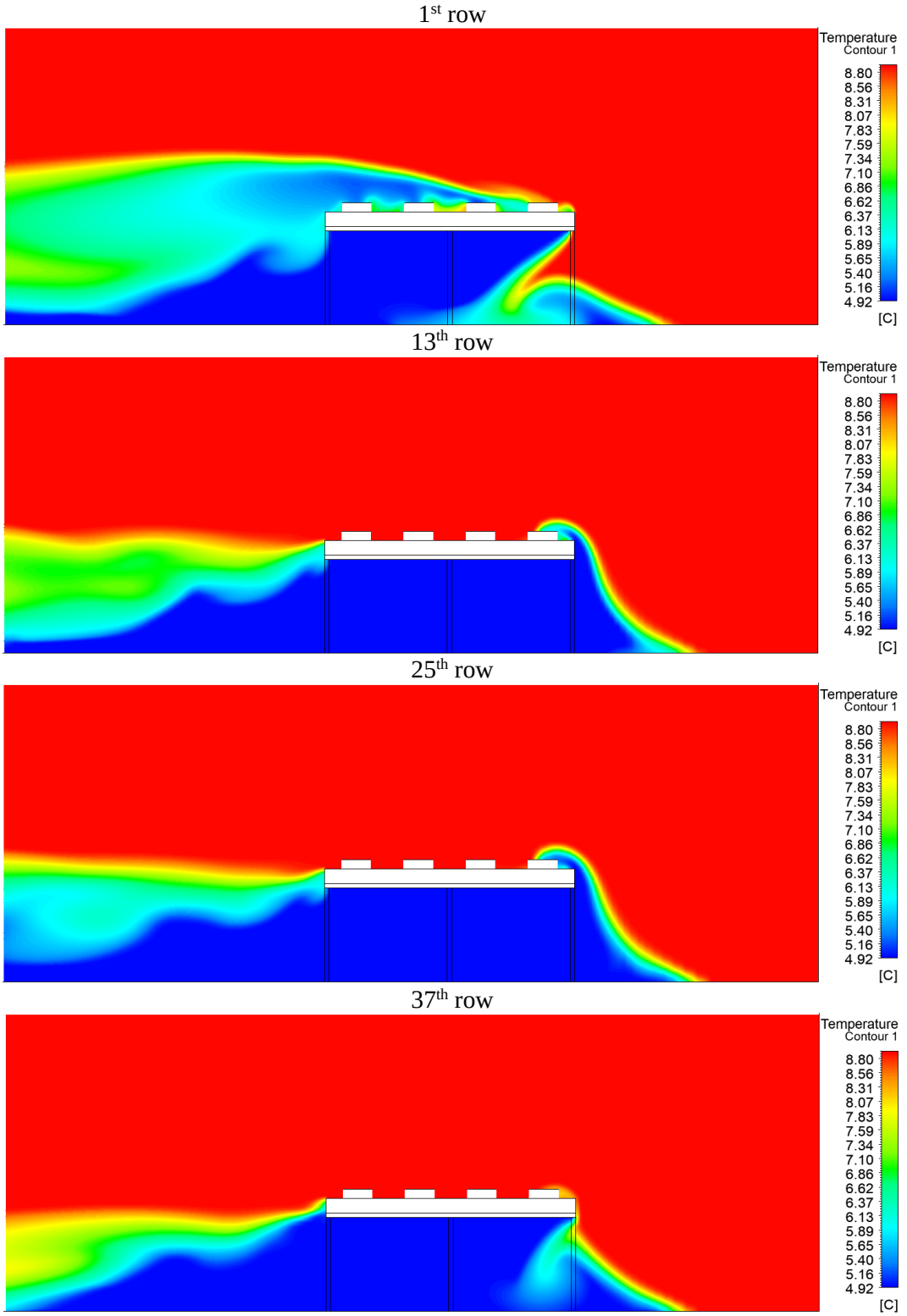

Figure 17. Temperature contour at different locations (rows) of the evaporators, for 20 evaporators and east wind condition

The corresponding temperature contour of the evaporators from above is shown in Figure 18.

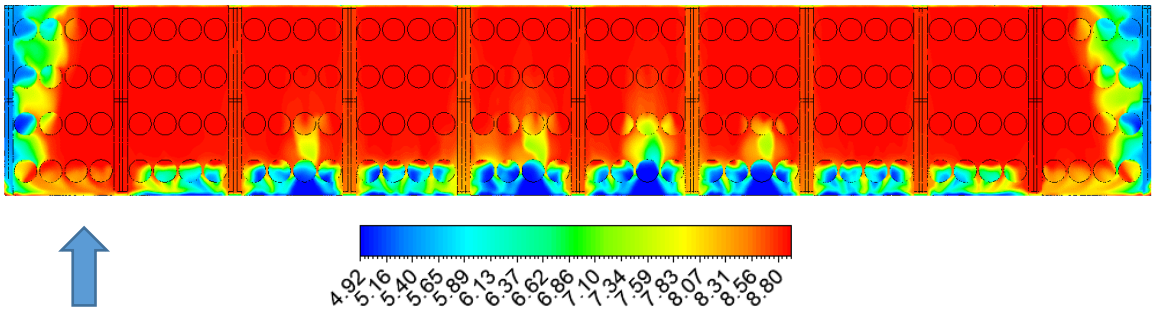

Figure 18. Temperature contour of the evaporators (top side), for 20 evaporators and east wind condition

With the corresponding local recirculation in Figure 19.

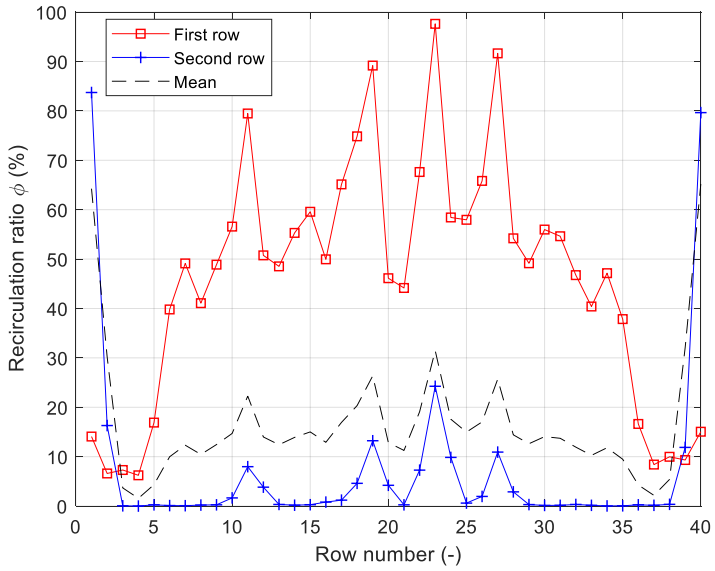

Figure 19. Local and mean recirculation at the intakes of the evaporators, for 20 evaporators and east wind

At some intakes, the recirculation is almost full, meaning that the temperature at the inlet of the heat exchanger is equal to the one at the outlet (locally). However, the recirculation drops at the second row, and with almost no recirculation for the 3rd and 4th row, except on the lateral sides. The local recirculation shows spikes due to the presence of the legs, which constitutes a full blockage of the main flow. The semi chaotic behaviour may be explained by the complex geometry and the inherent chaotic properties of turbulent flows. Overall, the average recirculation is equal to φ = 16.9%, which is lower than for the south wind condition.

3.3. South-East wind

In this cases, the wind attacks two sides of the evaporators. The velocity components are adjusted depending on the angle formed by the wind direction with the reference vector (south) by using basic trigonometric laws, see appendix A.

The temperature contour of the evaporators (top view) is shown in Figure 20 for all wind directions, including two new angles (7.5° and 15°) to cover a broader range of wind direction.

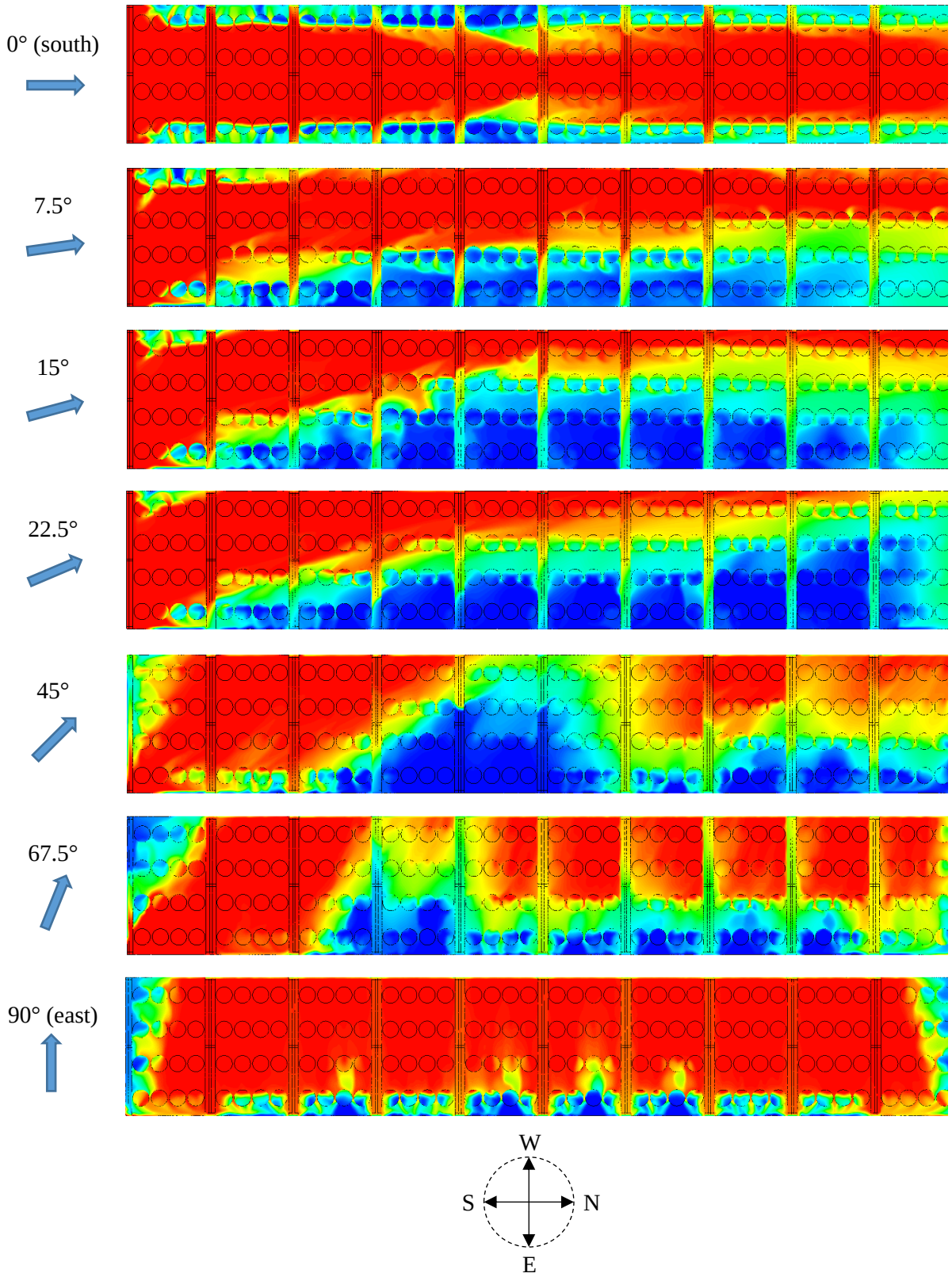

Figure 20. Temperature contour of the evaporators (top side), for 20 evaporators and all wind conditions

The corresponding global recirculation ratio for all wind directions is shown in Figure 21. The results have been extrapolated for 360° due to the two symmetry plans of the geometry.

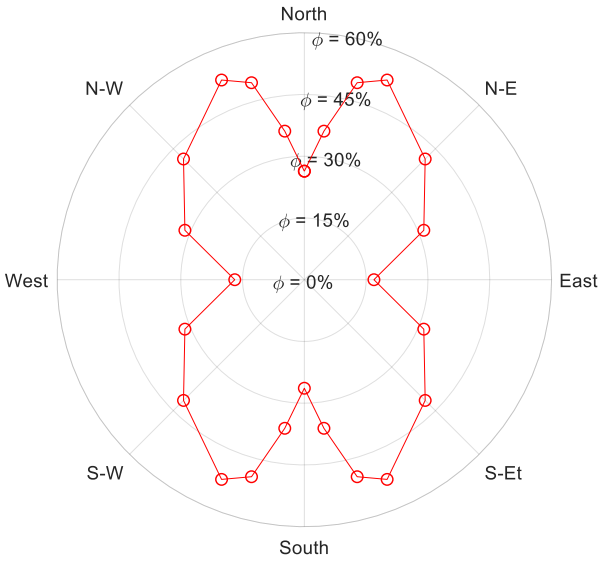

Figure 21. Global recirculation at the intakes of the evaporators, for all wind directions

The last two figures show that the recirculation is the lowest (φ = 16.9%) for west and east directions, and the highest (φ = 52.5%) for an angle of +/- 22.5° from the north or south direction. This high recirculation ratio can be explained by the combination of several factors:

- Taking the example in Figure 20, at small angle the wind does not have sufficient kinetic energy to entrain the exhaust flow in the west direction. Therefore, the exhaust flow has little resistance to flow upstream (in the east direction) and recirculates back the evaporator intakes,
- The wind will carry the exhaust flow towards the upper surface of the evaporators at the intakes, in combination with the "natural" recirculation by the lateral vortices.

On the other hand, for west and east wind, if the wind slightly changes its direction the recirculation does not drastically increase. Therefore, the evaporators have to be placed to have the wind coming from their sides in order to have a minimum recirculation ratio and limits the effect of the fluctuation of the wind direction.

4. Brædstrup test case with "real" field

ON GOING.

References

[1] J. Franke, A. Hellsten, H. Schlünzen, and B. Carissimo, *BEST PRACTICE GUIDELINE FOR THE CFD SIMULATION OF FLOWS IN THE URBAN ENVIRONMENT*. 2007.

[2] J. JEong and F. Hussain, “On the identification of a vortex,” *J. Fluid Mech.*, vol. 285, no. February, pp. 69–94, 1995.

Appendix A

Velocity inlet profile

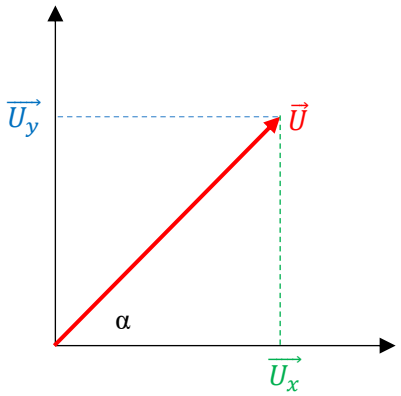

Projected velocity on x-axis

$$U_x = U \cdot \cos(\alpha)$$

Projected velocity on y-axis

$$U_y = U \cdot \sin(\alpha)$$